ELSEVIER

Materials Chemistry and Physics 60 (1999) 231–239

MATERIALS CHEMISTRY AND PHYSICS

Optical-constant calculation of non-uniform thickness thin films of the $Ge_{10}As_{15}Se_{75}$ chalcogenide glassy alloy in the sub-band-gap region (0.1–1.8 eV)

E. Márquez[a,*], A.M. Bernal-Oliva[a], J.M. González-Leal[a], R. Prieto-Alcón[a], A. Ledesma[a], R. Jiménez-Garay[a], I. Mártil[b]

[a]*Departamento de Física de la Materia Condensada, Facultad de Ciencias. Universidad de Cádiz, 11510 Puerto Real (Cádiz), Spain*
[b]*Departamento Electricidad y Electrónica, Facultad de Físicas, Universidad Complutense, 28040 Madrid, Spain*

Received 1 December 1998; received in revised form 23 March 1999; accepted 26 March 1999

Abstract

Optical-transmission spectra are very sensitive to inhomogeneities in thin films. In particular, a non-uniform thickness produces a clear shrinking in the transmission spectrum at normal incidence. If this deformation is not taken into account, it may lead to serious errors in the calculated values of the refractive index and film thickness. In this paper, a method first applied by Swanepoel for enabling the transformation of an optical-transmission spectrum of a thin film of wedge-shaped thickness into the spectrum of a uniform film, whose thickness is equal to the average thickness of the non-uniform layer, has been employed. This leads subsequently to the accurate derivation of the refractive index in the subgap region (0.1–1.8 eV), the average thickness, as well as a parameter indicating the degree of film-thickness uniformity. This optical procedure is applied to the particular case of freshly-prepared films of the $Ge_{10}As_{15}Se_{75}$ ternary chalcogenide glassy alloy. The dispersion of the refractive index is discussed in terms of the Wemple–DiDomenico single-oscillator model. The optical-absorption edge is described using the 'non-direct transition' model proposed by Tauc, and the optical energy gap is calculated by Tauc's extrapolation. Finally, the photo-induced and thermally induced changes in the optical properties of the *a*-$Ge_{10}As_{15}Se_{75}$ layers are also studied.

Keywords: Amorphous semi-conductors; Ternary chalcogenide glasses; Thin films; Optical constants; Thermally and photo-induced effects

1. Introduction

Chalcogenide glasses are well-known IR-transmitting materials [1], and exhibit a wide range of photo-induced effects that enable them to be used as optical recording or imaging media [2]. The accurate knowledge of their optical constants is necessary not only for understanding the basic mechanisms of these effects, but also for exploiting their interesting technological potentials.

Among the existing methods for determining the optical constants, those that are based exclusively on the optical-transmission spectra at normal incidence [3,4] have been applied to different crystalline and amorphous materials, deposited on transparent substrates, in the form of thin films, following different techniques [5–7]. These relatively simple methods, apart from being non-destructive and not needing any previous knowledge about the thickness of the deposited film, are fairly accurate — the thickness and refractive index can be determined with an accuracy of about 1% [4]. They do, however, assume a layer with uniform thickness; when the thickness is not uniform, a clear shrinking in the optical-transmission spectrum is produced, leading to less accurate final results and even serious errors.

In this work, a procedure first applied by Swanepoel [8] to inhomogeneous films of *a*-Si : H, which takes into account the profile of the layers, is systematically applied to $Ge_{10}As_{15}Se_{75}$ ternary chalcogenide glass films. The method is based on the transformation of the envelopes of the transmission spectrum corresponding to a film of non-uniform thickness, into the envelopes of the spectrum of a uniform film, whose thickness is equal to the average thickness of the non-uniform film: It allows the determination of the geometrical parameters, average thickness and thickness variation, and the refractive index. It should be

*Corresponding author. Tel.: +34-56-830966; fax: +34-56-834924; e-mail: emilio.marquez@uca.es

0254-0584/99/$ – see front matter
PII: S0254-0584(99)00078-4

emphasized that, by using the method presented here, it is possible to obtain accurate information about the non-uniform chalcogenide films under study, from a transmission spectrum that would otherwise be useless. In addition, the lack of data in the literature concerning the optical characterization of thin films of ternary chalcogenide glasses clearly highlights the significance of the present study. Finally, the changes of the optical constants of freshly-prepared *a*-$Ge_{10}As_{15}Se_{75}$ films, induced by both thermal annealing (in vacuum) and light exposure (in air), are also described.

2. Experimental details

Thin-film samples were deposited by vacuum evaporation of powdered melt-quenched glassy material (prepared by heating an appropriate mixture of the elements in a vacuum-sealed fused silica ampoule, for about 24 h, at approximately 900°C, and then air-quenching), onto CaF_2 glass substrates – transparent in the 0.1–4.1 eV spectral region. The thermal evaporation process was carried out in a coating system (Edwards, model E306A), at a pressure of $\approx 5 \times 10^{-7}$ Torr, from a suitable quartz crucible. During the deposition process the substrates were conveniently rotated by means of a rotary workholder, which makes it possible to relatively reduce the lack of uniformity in the thickness of the as-deposited glass films [9]. A schematic drawing of the experimental arrangement inside the coating system is displayed in Fig. 1(a). The deposition rate was ≈ 0.5 nm s^{-1}, which was measured continuously by a quartz-crystal monitor (Edwards, model FTM-5). It is known that such a low deposition rate produces a chemical composition, which is very close to that of the bulk starting material : Electron microprobe analysis indicated that the composition is correct to within ±1 at.%. The examination of the thin-film samples by scanning electron microscopy was carried out in an electron microscope (Jeol, model JSM-820). The result of the corresponding compositional analysis is presented as an inset in Fig. 1(b). The absence of crystallinity in the layers was verified by X-ray diffraction (XRD) measurements (using a Philips, model PW-1710 diffractometer). Fig. 1(b) also shows a typical XRD-pattern, using the Cu Kα line (1.54 Å), for a representative as-deposited $Ge_{10}As_{15}Se_{75}$ chalcogenide film.

One aspect of the diffraction results in chalcogenide materials has been ascribed to the influence of medium-range order, and this is the so-called first sharp diffraction peak (FSDP) or pre-peak in the structure factor [10]. This peak almost invariably occurs at a value of the modulus of the scattering vector of ≈ 1 $Å^{-1}$ in amorphous chalcogenides. The absence of FSDP in the ternary alloy under study is certainly noteworthy (this significant fact has also been found by El-Samanoudy and Fadel [11,12], with different amorphous $Ge_{25-x}As_xSe_{75}$ films), in clear contrast to the binary glassy alloy, $Ge_{25}Se_{75}$ (see Fig. 1(b)).

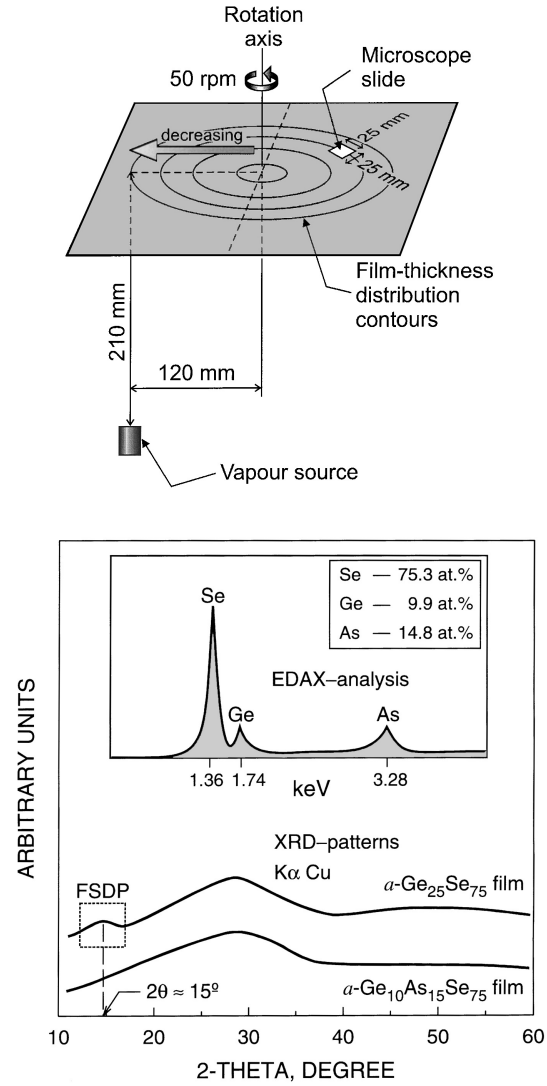

Fig. 1. (a) Diagram showing the experimental arrangement used in the thermal-evaporation process. It also shows the distribution of the film thickness in the rotary workholder, and the dimensions of a representative substrate. (b) XRD-(Cu Kα radiation) of an as-evaporated $Ge_{10}As_{15}Se_{75}$ chalcogenide glassy sample, and that corresponding to a layer of the $Ge_{25}Se_{75}$ binary alloy,showing the FSDP at $2\theta \approx 15°$, or equivalently, at a value of the modulus of the scattering vector, Q ($=4\pi\sin\theta/\lambda$) of $\approx$ 1.1 $Å^{-1}$. The inset shows the results of the corresponding compositional analysis.

The optical-transmission spectra were obtained over the 0.4–3.1 eV spectral region by a double-beam, UV/Vis/NIR computer-controlled spectrophotometer (Perkin–Elmer, model Lambda-19), while IR measurements over the 0.1–0.4 eV spectral region were carried out by a computer-controlled FTIR spectrometer (Perkin–Elmer, model 2000); the spectrophotometer allows the selection of two different light beam sizes (4 or 10 × 1 mm^2). In addition, a surface-profiling stylus (Sloan, model Dektak 3030) was used to measure the thickness of the layers for the purpose of comparison with the result derived from the optical measurements. The thicknesses studied in the present work were in the range of approximately 800–2000 nm. All the

optical measurements reported were made at room temperature.

3. Theoretical considerations

The optical-characterization method used in this work assumes that the thickness of the film varies linearly over the illuminated area, and can be expressed as: $d = \bar{d} \pm \Delta d$. This assumption is reasonable in the case of the present thermally-evaporated thin-film samples, because the film-thickness distribution over the substrate dimensions (around $25 \times 25\ mm^2$) is approximately in the shape of a wedge [9] (see Fig. 1(a) and the inset of Fig. 2);Δd refers to the actual variation in thickness from the average thickness $\bar{d}$. The upper and lower envelopes, T_M and T_m, respectively, of the transmission spectrum corresponding to a wedge-shaped layer, can be written as a function of the envelopes, T_{M0} and T_{m0}, of the uniform film with the same optical constants and thickness equal to the average thickness of the non-uniform film, as:

$$T_{M,m} = \frac{(T_{M0}T_{m0})}{\chi}\tan^{-1}\left[\left(\frac{T_{M0}}{T_{m0}}\right)^{\pm 1/2}\tan\chi\right] \quad (1)$$

where

$$\chi = \frac{2\pi n\Delta d}{\lambda} \quad (2)$$

verifying, $0 < \chi < \pi/2$ (or equivalently, $0 < \Delta d < \lambda/4n$).

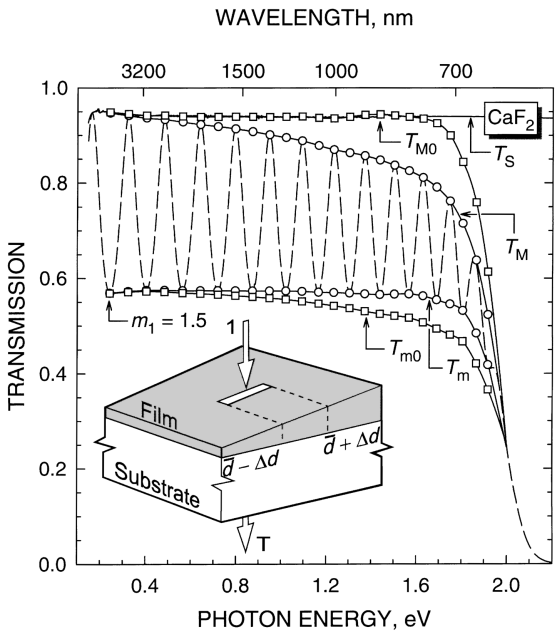

Fig. 2. Optical transmission versus photon energy corresponding to a wedge-shaped film of the $Ge_{10}As_{15}Se_{75}$ ternary alloy, deposited onto a thick, transparent CaF_2 substrate. T_{M0}, T_M, T_m and T_{m0} are defined in the text, and T_s is the transmission of the substrate alone. Also, a schematic drawing of a weakly-absorbing film, with a linear variation in thickness, on a transparent substrate.

Once both envelopes, T_M and T_m, are known, the expressions included in Eq. (1) are two independent transcendental equations for T_{M0}, T_{m0}, and χ. Considering that in the transparent region $T_{M0} \equiv T_s$, where T_s is the transmission of the substrate alone (see Fig. 2), the two expressions in Eq. (1) can be solved for T_{m0} and χ in this particular spectral region, using a rapidly-converging algorithm (Newton–Raphson iteration). In addition, the well-known equation for the interference fringes, $2n\bar{d} = m\lambda$ (m being the order number), which, due to the optical absorption, is verified at the tangent points between the envelopes and the optical-transmission spectrum, is now used to calculate T_{M0} and T_{m0} over the whole spectral range under study. This equation can be rewritten as [4,8]:

$$\frac{l}{2} = \frac{2n\bar{d}}{\lambda} - m_1. \quad (3)$$

where $l = 0,1,2,3,\ldots$ for the successive tangent points, starting from the long-wavelength end, and m_1 is the order number of the first ($l = 0$) tangent point considered, while m_1 is an integer or a half-integer, for the upper or lower tangent points, respectively. The substitution of Eq. (2) in Eq. (3) gives:

$$\frac{l}{2} = \left(\frac{\bar{d}}{\pi\Delta d}\right)\chi - m_1. \quad (4)$$

A plot of $l/2$ as a function of χ in the transparent region allows the determination of the slope and m_1, based on Eq. (4), which is illustrated in Fig. 3. Eq. (4) can be used for the calculation of χ for the tangent points in the region of absorption, and T_{M0} and T_{m0} can then be derived from Eq. (1), as discussed below in detail. Once the values of T_{M0} and T_{m0} are known, we can optically characterize the non-uniform chalcogenide films by the application of a procedure corresponding to uniform layers [4,8,13].

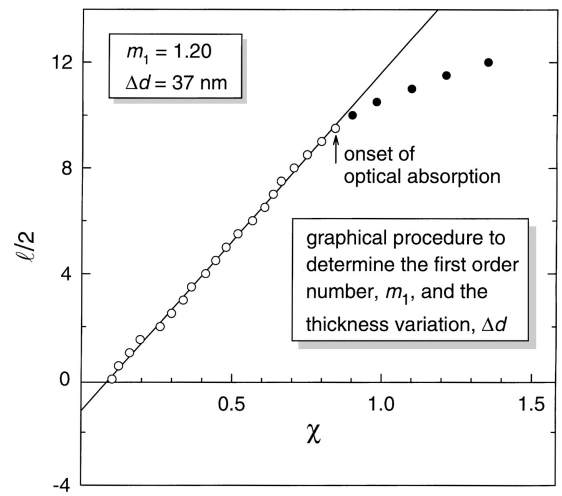

Fig. 3. Plot of $l/2$ as a function of χ, in order to determine m_1 and Δd for the representative $Ge_{10}As_{15}Se_{75}$ thin-film sample.

4. Results and discussion

4.1. Determining the refractive index and average film thickness

Fig. 2 presents the experimental optical transmission as a function of the photon energy, corresponding to a representative wedge-shaped thin film of the $Ge_{10}As_{15}Se_{75}$ glassy alloy. It can be seen from this curve that using the photon-energy axis, the adjacent extrema are at approximately the same distances from each other, i.e., $\Delta(\hbar\omega)^{ext} = (\hbar\omega)^{ext}_{i+1} - (\hbar\omega)^{ext}_{i} \approx$ constant. Due to the optical dispersion ($n = n(\hbar\omega)$), a slight decrease of $\Delta(\hbar\omega)^{ext}$ is however observed with increasing photon energy ($\Delta(\hbar\omega)^{ext} =$ constant, for the non-dispersive case). This figure also clearly shows the non-uniformity of thickness of the *a*-$Ge_{10}As_{15}Se_{75}$ ternary films used in the present study. The experimental envelopes, T_M and T_m, presented in Fig. 2, have been carefully drawn using a computer program devised by McClain et al. [14]. In addition, the transmission of the CaF_2 substrate alone is included in Fig. 2, as T_s.

As it has already been explained, T_{m0} and χ are calculated initially from Eq. (1), using the experimental values of T_M and T_m for the tangent points, and substituting $T_{M0} = T_s$. Fig. 3 shows the plot of $l/2$ as a function of χ according to Eq. (4), while the best straight-line fit for the points of the transparent region is also drawn. The points for larger χ, which clearly deviate from this straight line, indicate the onset of absorption and these points have to be ignored when the straight line is drawn. The equation corresponding to this particular straight line is:

$$\frac{l}{2} = 12.85\chi - 1.20. \tag{5}$$

New values of χ can be calculated for each tangent point, over the whole spectral range, using a new expression derived by modifying the above equation, in such a way that the particular value of m_1 is appropriately rounded off (in this case, $m_1 = 1.5$). T_{M0} and T_{m0} are now calculated from Eq. (1), using these new values of χ, and the values of T_M and T_m; the experimental values of T_M and T_m at the tangent points, as well as the calculated values of T_{M0} and T_{m0}, for the same photon energies, are all displayed in Fig. 2.

The values of T_{M0} and T_{m0} can now be used to a derive $\bar{d}$ and $n(\hbar\omega)$ using, as previously mentioned, the method for uniform films. The value of the average thickness for the representative thin-film sample is 1488 ± 13 nm (the accuracy of this final value of the average thickness is 0.9%). In addition, substituting the value of $\bar{d}$ in Eq. (4) and using the value of the slope corresponding to Eq. (5), gives a value for Δd of $\approx$37 nm. Alternatively, the film thickness was measured directly by the previously-mentioned Sloan Dektak 3030 mechanical profilometer. This measured value is usually very close to that calculated by the envelope-curve procedure. The difference between the directly-measured value of thickness, 1476 ± 30 nm, and the optically-calculated value is +0.8%.

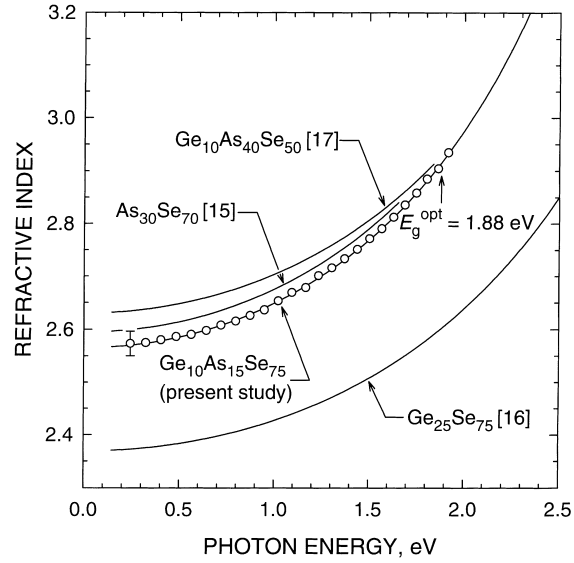

Fig. 4. Refractive index versus photon energy in the sub-band-gap region, for the as-deposited *a*-$Ge_{10}As_{15}Se_{75}$ film, in comparison with the same plot for the $As_{30}Se_{70}$, $Ge_{25}Se_{75}$ and $Ge_{10}As_{40}Se_{50}$ chalcogenide glass layers.

The final values of the refractive index in the subgap region (0.1–1.8 eV), for the representative non-uniform film of the $Ge_{10}As_{15}Se_{75}$ chalcogenide alloy, are displayed in Fig. 4, as a function of the photon energy. The corresponding dispersion curve, $n(\hbar\omega)$, which is also shown in Fig. 4, has been plotted using the dispersion relationship that will be introduced below. Moreover, the dispersion curves obtained from the optical-dispersion parameters reported in the literature, for the binary alloys $As_{30}Se_{70}$ [15] and $Ge_{25}Se_{75}$ [16], and for the ternary alloy $Ge_{10}As_{40}Se_{50}$ [17], are also shown in Fig. 4 for comparison.

4.2. Determining the absorption coefficient and optical band gap

Concerning the procedure for the determination of the absorption and extinction coefficients, Swanepoel [4] recommends that, in the case of uniform films, the T_{M0}-curve should be used over the whole range of the spectrum, namely in the regions of strong, medium and weak absorption. It is stressed that the T_{M0}-curve displayed in Fig. 2 has been computer drawn by interpolation of a cubic spline, through the calculated T_{M0}-values. The derivation of the optical absorbance, x, is based on the expression for the optical dispersion that will be presented later. The corresponding formula for the calculation of x is:

$$x = \frac{E_{M0} - [E_{M0}^2 - (n^2-1)^3(n^2-s^4)]^{1/2}}{(n-1)^3(n-s^2)}, \tag{6}$$

where

$$E_{M0} = \frac{8n^2 s}{T_{M0}} + (n^2 - 1)(n^2 - s^2). \quad (7)$$

The absorption coefficient, α, is then calculated, using the relationship: $\alpha = -(1/\bar{d}) \ln x$. Once α is known, the extinction coefficient, k, can be easily determined from the above-mentioned relationship, $k = \alpha\lambda/4\pi$, which completes the derivation of the two optical constants (n, k). Moreover, in the region where the interference fringes disappear (see Fig. 2), and the curves T_{M0} and T_{m0} converge to a single curve, T_0, the following expression can be written [4]:

$$T_0 \approx \frac{Ax}{B}, \quad (8)$$

and, thus,the optical absorbance can be also determined in the region of strong absorption by:

$$x \approx \frac{(n+1)^3(n+s^2)}{16n^2 s} T_0. \quad (9)$$

The optical-absorption spectrum and the corresponding plot of the extinction coefficient versus photon energy, obtained by using Eq. (6), are both displayed in Fig. 5 for the present representative, as-deposited thin-film sample of the $Ge_{10}As_{15}Se_{75}$ alloy. Furthermore, the values of the absorption coefficient for the $As_{30}Se_{70}$ [15] and $Ge_{25}Se_{75}$ [16] binary compositions, as well as the corresponding optical-absorption edge for the same ternary composition under study, reported by El-Samanoudy and Fadel [11], are also shown in Fig. 5, for the purpose of comparison.

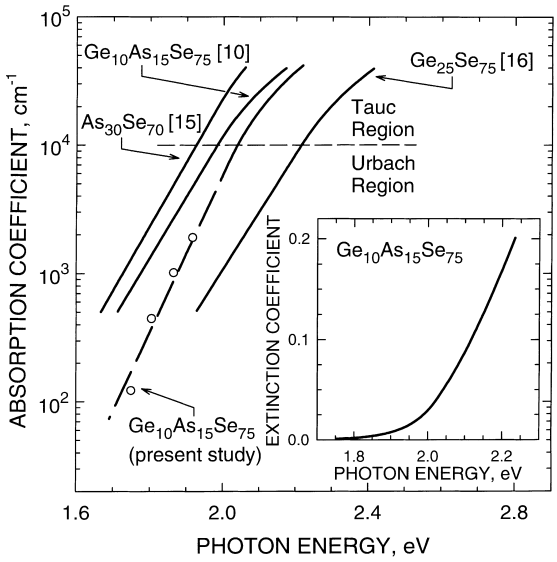

Fig. 5. Optical-absorption edge for the representative $Ge_{10}As_{15}Se_{75}$ sample, and the corresponding absorption edges for the $As_{30}Se_{70}$ and $Ge_{25}Se_{75}$ binary alloys. Also shown is the absorption edge taken from [11], for the same ternary chalcogenide composition studied in this work. The inset shows the extinction coefficient, k, as a function of photon energy.

In the strong-absorption region, involving inter-band optical transitions between valence and conduction bands, α is given according to Tauc [18], by the equation:

$$\alpha(\hbar\omega) = \frac{B(\hbar\omega - E_g^{opt})^2}{\hbar\omega}, \quad (10)$$

where E_g^{opt} is the optical gap and B is a constant, which is a measure of the extent of band tailing. It is related to the width of the band tails, ΔE_{tail}, by the following expression [19]:

$$B = \frac{4\pi\sigma_{min}}{n_0 c \Delta E_{tail}}, \quad (11)$$

where σ_{min} is the minimum metallic conductivity, n_0 the static refractive index and c the light velocity.

The values of E_g^{opt} and B can be readily derived by plotting $(\alpha\hbar\omega)^{1/2}$ as a function of $\hbar\omega$. Fig. 6 shows this curve for the representative $Ge_{10}As_{15}Se_{75}$ sample and for the rest of the chalcogenide alloys shown previously in Fig. 5. On the other hand, Table 1 shows the values of the Tauc gap, E_g^{opt}, and the Tauc slope, $B^{1/2}$, along with the values of the alternative optical gaps, E_{04} and E_{03}, which represent the energy at which the absorption coefficient reaches the values of 10^4 and 10^3 cm^{-1}, respectively. From the different values of the optical gaps listed in Table 1, it is deduced that all these gaps increase with increasing Ge-content, which can be clearly explained by the fact that the Ge–Se bonds have a much higher binding energy (473 kJ mol^{-1}) than that of the As–Se bonds (96 kJ mol^{-1}), and this obviously leads to much higher splitting between the valence and conduction band states. Also, from the Tauc slope, $B^{1/2} = 904$ cm$^{-1/2}$ eV$^{-1/2}$, the static refractive index, $n_0 = 2.566$, which will be later derived, and $\sigma_{min} \approx 300\ \Omega^{-1}$ cm^{-1} [20], Eq. (11) can be solved to give

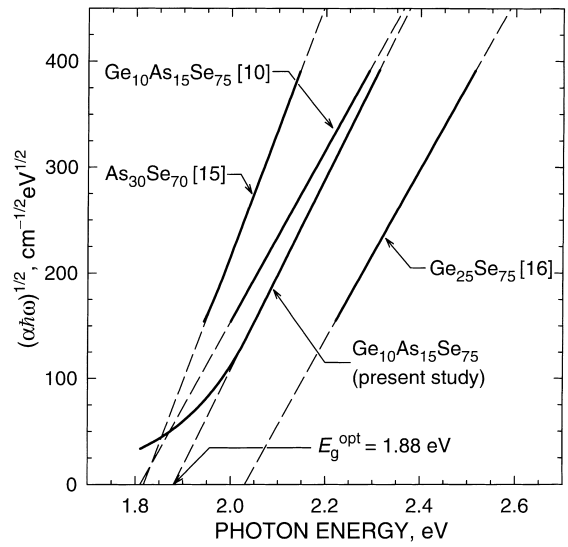

Fig. 6. Determination of the optical band gap, E_g^{opt}, in terms of the Tauc law.

Table 1
Values of the single-oscillator energy or Wemple–DiDomenico 'gap' (E_0), dispersion energy (E_d), static refractive index (n_0), Tauc gap (E_g^{opt}) and slope ($B^{1/2}$); the scatters of these optical parameters have been directly derived from those obtained by the corresponding least-squares fits. Also, two alternative options, very often used, for the optical gap (E_{04} and E_{03}), the slope parameter (E_e) and the pre-exponential factor (α_0), these two last parameters associated to the Urbach region, are all listed in this table.

Chalcogenide alloy	E_0 (eV)	E_d (eV)	n_0	$B^{1/2}$ ($cm^{-1/2}$ $eV^{-1/2}$)	E_g^{opt} (eV)	E_{04} (eV)	E_{03} (eV)	E_e (meV)	α_0 $(cm)^{-1}$
$As_{30}Se_{75}$ [15]	3.79	21.81	2.600	1321	1.82	1.92	1.80	54	–
$Ge_{10}As_{15}Se_{75}$ [11]	–	–	–	811	1.81	2.14	–	217	–
$Ge_{10}As_{15}Se_{75}$	3.72 ± 0.01	20.77 ± 0.5	2.566 ± 0.001	904 ± 1	1.88 ± 0.01	2.04 ± 0.01	1.87 ± 0.01	71 ± 1	3×10^{-9}
$Ge_{25}Se_{75}$ [16]	4.21	19.43	2.369	806	2.03	2.21	1.99	80	–

an approximate estimate of the width of the band tails, $\Delta E_{tail} \approx 68$ meV, for $Ge_{10}As_{15}Se_{75}$ film.

Continuing with the analysis of the optical-absorption edge, at lower values of the absorption coefficient ($1\ cm^{-1} < \approx \alpha < \approx 10^4\ cm^{-1}$), the absorption depends exponentially on photon energy, according to the so-called Urbach's relationship [19] (see Fig. 5):

$$\alpha(\hbar\omega) = \alpha_0 \exp\left(\frac{\hbar\omega}{E_e}\right) \tag{12}$$

where E_e is a slope parameter, typically having values in the range 40–100 meV. Furthermore, E_e is generally considered to represent the randomness of the glass structure. It should be pointed out that, for values of $\alpha < \approx 10^3\ cm^{-1}$, there is a significant decrease in the accuracy of the α-values obtained from the optical-transmission measurements. The value for the slope parameter, E_e, obtained from the corresponding α-values, is ≈71 meV.

Finally, it should be mentioned that there is a difference of ≈4% between the Tauc gap derived in the present study, and that reported by El-Samanoudy and Fadel [11] for layers of the same chemical composition, 1.81 eV. This difference could be explained considering that in [11], the calculation of the absorption coefficients is carried out only approximately, by use of the well-known Lambert–Beer law: $I = I_0 \exp(-\alpha d)$, where I and I_0 are the intensities of the transmitted and incident beams, respectively. However, this expression does not take into account, obviously, the multiple reflections at the three interfaces of the optical system analyzed, which can lead to serious errors in the values obtained for α.

4.3. Analysis of the optical dispersion based on the Wemple-DiDomenico single-oscillator framework

The refractive-index dispersion, $n(\hbar\omega)$, of crystalline and amorphous materials can be fitted by the Wemple–DiDomenico relationship [21,22]:

$$n^2(\hbar\omega) = 1 + \frac{E_d E_0}{E_0^2 - (\hbar\omega)^2}, \tag{13}$$

where E_0 and E_d are single-oscillator fitting constants, which measure the oscillator energy and strength, respectively. The oscillator energy, E_0, is an 'average' energy gap, and it scales with the Tauc gap, E_g^{opt}, i.e., $E_0 \approx 2 \times E_g^{opt}$, as it was found by Tanaka [23] investigating well-annealed As-S chalcogenide glass films, and also verified with other amorphous chalcogenide materials [24–26]. Furthermore, E_d obeys a simple empirical expression [21,22]:

$$E_d = \beta N_c Z_a N_e (\text{eV}), \tag{14}$$

where $\beta \approx 0.4$ eV for covalent crystalline and amorphous materials (with $\beta \approx 0.3$ eV for ionic materials), N_c is the coordination number of the cation nearest-neighbour to the anion, Z_a is the formal chemical valency of the anion, and N_e is the total number of valence electrons (cores excluded) per anion.

By plotting $(n^2 - 1)^{-1}$ as function of $(\hbar\omega)^2$ and fitting a straight line as shown in Fig. 7, E_0 and E_d can be determined directly from the slope, $(E_0 E_d)^{-1}$, and the intercept on the vertical axis, E_0/E_d, respectively. The straight-line equation corresponding to the least-squares fit is: $(n^2-1)^{-1} = 0.1790 - 0.0129\ (\hbar\omega)^2$, with a value of the correlation coefficient of 0.9996. Also, in Table 1 are listed the values

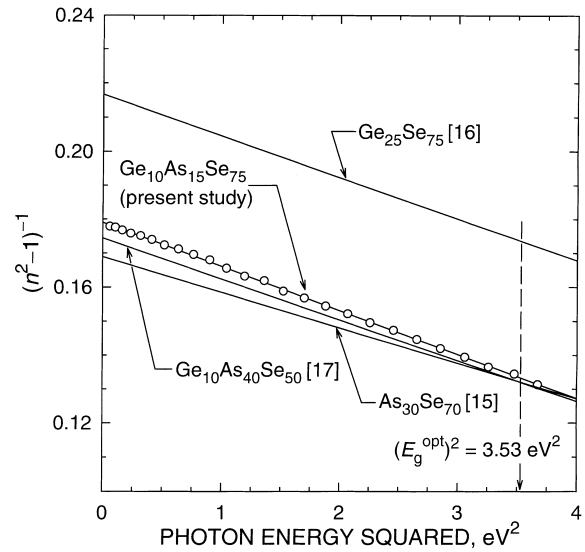

Fig. 7. Plot of the refractive-index factor $(n^2-1)^{-1}$ versus $(\hbar\omega)^2$, for determination of the Wemple–DiDomenico dispersion parameters, E_0 and E_d, for the case of a $Ge_{10}As_{15}Se_{75}$ glass film, in comparison with the same plot for the $As_{30}Se_{70}$, $Ge_{25}Se_{75}$ and $Ge_{10}As_{40}Se_{50}$ chalcogenide layers.

obtained for the Wemple–DiDomenico dispersion parameters, E_0 and E_d, and the value of the static refractive index (calculated extrapolating the Wemple–DiDomenico optical-dispersion equation to $\hbar\omega \rightarrow 0$), n_0, for the representative sample of the $Ge_{10}As_{15}Se_{75}$ alloy, as well as for the $As_{30}Se_{70}$ [15] and $Ge_{25}Se_{75}$ [16] binary alloys.

From the Wemple's empirical expression for the dispersion energy, E_d, mentioned above, a cation-coordination number, N_c, can be estimated using the relationship: $N_c = E_d/\beta Z_a N_e$, where, in this particular case, $Z_a = 2$ and $N_e = (4 \times 10 + 5 \times 15 + 6 \times 75)/75 = 113/15$. Thus, $N_c \approx 3.45$. This value is certainly in excellent agreement with that which would be expected for the $Ge_{10}As_{15}Se_{75}$ chalcogenide glass. In fact, if we rewrite this chemical composition in the following form: $(Ge_{0.4}As_{0.6})_{25}Se_{75}$, a hypothetical 'cation' such as $Ge_{0.4}As_{0.6}$ could now be considered. For this 'cation', N_c could be obtained as follows: $N_c^{theo} = 4 \times 0.4 + 3 \times 0.6 = 3.40$. For a general glassy composition $Ge_xAs_ySe_z$, if only heteropolar chemical bonds are considered, the expression: $4x + 3y = 2z$, should be verified. Then, taking the value $N_c^{theo} = 3.40$ that we have previously derived, this last equation leads to a composition such as $Ge_{15}As_{22}Se_{63}$, which clearly indicates the necessary presence of homopolar chemical bonds in the material under study.

Furthermore, an approximate value of the optical band gap, E_g^{opt}, can also be derived from the Wemple–DiDomenico dispersion parameter, E_0, according to the already mentioned expression, $E_g^{opt} \approx E_0/2$, giving an alternative value of E_g^{opt} of $\approx 1.86 \pm 0.01$ eV. This value is in very good agreement with that determined from the Tauc's extrapolation, 1.88 ± 0.01 eV.

4.4. Thermally and optically induced changes of the optical properties

Freshly-prepared *a*-$Ge_{10}As_{15}Se_{75}$ films were annealed at around 133 °C (the value of the glass transition temperature, T_g, corresponding to the bulk glassy material is ≈ 143°C, and it was determined by a Perkin–Elmer differential scanning calorimeter, model System-8), for period of time of about 24 h, in a $\approx 10^{-3}$ Torr vacuum. As a consequence of the thermal-annealing process, the Tauc gap increases up to 1.93 ± 0.01 eV ($\Delta E_g^{opt} = +0.05$ eV), i.e., a thermal-bleaching effect takes place. A similar variation in E_g^{opt} has been found for films of the $Ge_xAs_{25-x}Se_{75}$ ternary glassy system [11]. The increase in the value of the Tauc gap has been explained by the layers undergoing some atomic rearrangement during the annealing treatment [27]: Some defects are removed which, by reducing the density of dangling bonds, re-distribute atomic distances and bond angles and, thus, E_g^{opt} increases. Moreover, the optical dispersion parameters E_0 and E_d both increase when the $Ge_{10}As_{15}Se_{75}$ films studied are annealed ($E_0 = 3.91 \pm 0.02$ eV and $E_d = 21.93 \pm 0.07$ eV).

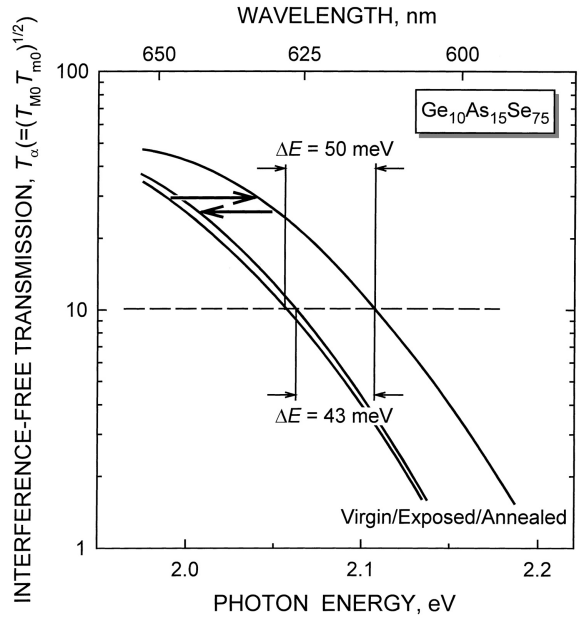

Fig. 8. Spectral dependence of the smooth interference-free transmission curve, T_α, which is defined as the geometric mean of T_{M0} and T_{m0} [4]; the values of the shift of the short-wavelength edge, ΔE, for the cases of thermal annealing and light exposure, are also presented.

Next, the annealed $Ge_{10}As_{15}Se_{75}$ films were illuminated (in air) for about 6 h, using a 500 W Hg arc lamp (Oriel, model 6285), with a light intensity of $\approx$ 30 mW cm^{-2} (which was measured by a thermopile). As a consequence of the light exposure the parameters E_g^{opt}, E_0 and E_d all decrease ($E_g^{opt} = 1.89 \pm 0.01$ eV, $E_0 = 3.80 \pm 0.03$ eV and $E_d = 21.03 \pm 0.10$ eV) and, equivalently, a photo-darkening phenomenon takes place: This can be explained in terms of the photo-induced scission and weakening of intermolecular bonds, which could lead to an increase in the intermolecular distances [28]. Fig. 8 shows the shifts in the interference-free transmission curve, T_α, as a consequence of the annealing and illumination of the *a*-$Ge_{10}As_{15}Se_{75}$ films. On the other hand, the refractive index of the $Ge_{10}As_{15}Se_{75}$ films increases upon thermal annealing ($n_0 = 2.571 \pm 0.001$), whereas as a consequence of the irradiation it decreases ($n_0 = 2.556 \pm 0.001$). The changes found in the values of the oscillator energy and strength, E_0 and E_d, due to first thermal annealing and then bandgap illumination, clearly agree with those reported by De Neufville et al. [17], for chalcogenide layers of the chemical composition $Ge_{10}As_{40}Se_{50}$. It is interesting to note that, the increase in the dispersion energy after the thermal-annealing process, leads to an increase in the cation-coordination number ($N_c = 3.64$). This result could be explained in terms of a thermal-densification phenomenon [27–29], that causes a clear diminution of the interstitial volume around cation-centered structural units and, thus, an increase in the interaction between structural layers. This explanation is certainly consistent with the decrease found in the film thickness ($\approx -2\%$). On the other hand, the decrease in

the cation-coordination number, as a consequence of the bandgap illumination of the well-annealed $Ge_{10}As_{15}Se_{75}$ films ($N_c = 3.49$), could be an indication of a photo-expansion effect [28], which is, indeed, consistent with the increase found in the thickness ($\approx +1\%$). Finally, it should be pointed out that, changes in the optical properties of aged (more than 6-months old) $Ge_{10}As_{15}Se_{75}$ films, have not been found [30].

5. Concluding remarks

Optical-transmission spectra of thermally-evaporated $Ge_{10}As_{15}Se_{75}$ films have been carefully measured using a UV/Vis/NIR spectrophotometer and a FTIR-spectrometer, which allow us to study a wide spectral region (0.1–2.5 eV); CaF_2 substrates were chosen because of their good transparency also over the wide spectral range studied. The procedures used in this work for calculating the average thickness and the optical constants of wedge-shaped layers of the $Ge_{10}As_{15}Se_{75}$ ternary alloy, have been successfully applied to layers whose average thicknesses ranged from around 800 to 2000 nm. The non-uniformity of the thickness found under the present deposition conditions, gives rise to a clear shrinking of the interference fringes of the transmission spectrum at normal incidence; inaccuracies and even serious errors certainly occur if n, $\bar{d}$ and α are calculated from such a shrunken transmission spectrum, under the unrealistic assumption that the film is uniform.

The method applied in this study makes it possible to derive the refractive index and average thickness to an accuracy better than 1%. The values of the average thickness and thickness variation, $\bar{d}$ and Δd, were cross-checked with those measured using the mechanical stylus instrument: Excellent agreement between the directly-measured and the optically-calculated values has been generally found. Moreover, all these results have been clearly corroborated using an independent optical-characterization method for non-uniform thickness thin films, also proposed by Swanepoel [8,30,31]. The subsequent fitting of the experimental values of the refractive index to the Wemple–DiDomenico single-oscillator model, results in optical-dispersion parameters directly related to the disordered structure of the chalcogenide material. Very significantly, from the above-mentioned Wemple's empirical expression for the dispersion parameter E_d, a cation-coordination number, $N_c \approx 3.45$, is derived.

The optical absorption spectra of the $Ge_{10}As_{15}Se_{75}$ glass thin films are fitted, in the strong absorption region, to the 'non-direct transition' model proposed by Tauc, as well as to the Urbach's rule in the medium and weak absorption regions. Furthermore, an increase of the slope parameter E_e, with Ge-content, is deduced from the present study, in contrast to the results reported by El-Samanoudy and Fadel [11]; our results suggest that the degree of structural disorder in the $Ge_xAs_{25-x}Se_{75}$ ternary system increases in line with the germanium content in the chalcogenide glasses. Also, the Tauc gap increases with increasing germanium content.

Lastly, the changes found in the optical properties, first on thermal annealing, and then on light exposure of the well-annealed samples, are certainly consistent with those reported by other authors [11,17]. The reproducibility found for all the optical parameters, after successive annealing-illumination cycles, could be taken as unambiguous proof of the existence of a reversible photo-darkening phenomenon.

Acknowledgements

The authors are grateful to Prof. R. Swanepoel (Rand Afrikaans University, Johannesburg, South Africa), Dr. L. Tichý (Joint Laboratory, Pardubice, Czech Republic) and Dr. M. McClain (National Institute of Standards and Technology, Gaithersburg, USA) for some very valuable discussions. Also, the authors would like to thank Mr. Royston Snart for his English language assistance. This work was supported by the CICYT (Spain), under the MAT 98-0791 project.

References

[1] J.A. Savage, Infrared Optical Materials and Their Antireflection Coatings, Hilger, London, 1985.
[2] A.E. Owen, A.P. Firth, P.J.S. Ewen, Philos. Mag. B. 52 (1985) 347.
[3] J.C. Manifacier, J. Gasiot, J.P. Fillard, J. Phys. E: Sci. Instrum. 9 (1976) 1002.
[4] R. Swanepoel, J. Phys. E: Sci. Instrum. 16 (1983) 1214.
[5] M. Hamman, M.A. Harith, W.H. Osman, Solid State Commun. 59 (1986) 271.
[6] J.A. Kalomiros, J. Spyridelis, Phys. Status Solidi (a) 107 (1988) 633.
[7] E. Márquez, J.B. Ramírez-Malo, P. Villares, R. Jiménez-Garay, P.J.S. Ewen, A.E. Owen, J. Phys. D: Appl. Phys. 25 (1992) 535.
[8] R. Swanepoel, J. Phys. E: Sci. Instrum. 17 (1984) 896.
[9] R. Glang, Handbook of Thin Film Technology, McGraw-Hill, New York, 1983, p. 1–55.
[10] S.C. Moss, D.L. Price, Physics of Disordered Materials, Plenum, New York, 1985, p. 77.
[11] M.M. El-Samanoudy, M. Fadel, J. Mater. Sci. 27 (1992) 646.
[12] M. Fadel, Vacuum 48 (1997) 73.
[13] J.B. Ramírez-Malo, E. Márquez, P. Villares, R. Jiménez-Garay, Mater. Lett. 17 (1993) 327.
[14] M. McClain, A. Feldman, D. Kahamer, X. Ying, Comput. Phys. 5 (1990) 45.
[15] C. Corrales, Ph.D. Thesis, University of Cádiz, 1995.
[16] J. Reyes, E. Márquez, J.B. Ramírez-Malo, C. Corrales, J. Fernández-Peña, P. Villares, R. Jiménez-Garay, J. Mater. Sci. 30 (1995) 4133.
[17] J.P. de Neufville, R. Seguin, S.C. Moss, S.R. Ovshinsky, Amorphous and Liquid Semiconductors, Taylor and Francis, London, 1974, p. 737.
[18] J. Tauc, A. Menth, J. Non-Cryst. Solids 8–10 (1972) 569.
[19] N.F. Mott, E.A. Davis, Electronic Process in Non-Crystalline Materials, Clarendon Press, Oxford, 1979, p. 289.
[20] P. Nagels, E. Sleeckx, R. Callaerts, E. Márquez, J.M. González, A.M. Bernal-Oliva, Solid State Commun. 102 (1997) 539.

[21] S.H. Wemple, M. DiDomenico, Phys. Rev. B. 3 (1971) 1338.
[22] S.H. Wemple, Phys. Rev. B 7 (1972) 3767.
[23] Ke. Tanaka, Thin Solid Films 66 (1980) 271.
[24] A.M. Bernal-Oliva, E. Márquez, J.M. González-Leal, A.J. Gámez, R. Prieto-Alcón, R. Jiménez-Garay, J. Mater. Sci. Lett. 16 (1997) 665.
[25] J. Ruíz-Pérez, E. Márquez, D. Minkov, J. Reyes, J.B. Ramírez-Malo, P. Villares, R. Jiménez-Garay, Phys. Scripta 53 (1996) 76.
[26] J.B. Ramírez-Malo, E. Máraquez, C. Corrales, P. Villares, R. Jiménez-Garay, Mat. Sci. Eng. B-Solid 25 (1994) 53.
[27] A. Zakery, A. Zekak, P.J.S. Ewen, C.W. Slinger, A.E. Owen, J. Non-Cryst. Solids 114 (1989) 109.
[28] S.R. Elliott, J. Non-Cryst. Solids 81 (1986) 71.
[29] S. Rajagopalan, K.S. Harshavardhan, L.K. Malhotra, K.L. Chopra, J. Non-Cryst. Solids 50 (1982) 29.
[30] J.M. González-Leal, A. Ledesma, A.M. Bernal-Oliva, R. Prieto-Alcón, E. Márquez, J.A. Angel, J. Carábe, Mater. Lett., 39 (1999) 232.
[31] J.B. Ramírez-Malo, C. Corrales, E. Márquez, J. Reyes, J. Fernández-Peña, P. Villares, R. Jiménez-Garay, Mater. Chem. Phys. 40 (1995) 30.